Modelling the effects of pore-water chemistry on the behaviour of unsaturated clays

Xiaoqin Lei [1,2,3,b], Henry Wong [2,a], Antonin Fabbri [2], Ali Limam [3] and Y. M. Cheng [4]

[1] *Key Lab Mt Hazards & Earth Surface Proc, Inst Mt Hazards & Environm, CAS, Chengdu, China*
[2] *Université de Lyon/ENTPE/LGCB-LTDS (UMR CNRS 5513), Vaulx en Velin, France*
[3] *Université de Lyon/INSA Lyon/LGCIE, Villeurbanne, France*
[4] *Department of Civil and Environmental Engineering, Hong Kong Polytechnic University*

Abstract. Due to their various applications in geo-environmental engineering, such as in landfill and nuclear waste disposals, the coupled chemo-hydro-mechanical analysis of expansive soils has gained more and more attention recently. These expansive soils are usually unsaturated under field conditions; therefore the capillary effects need to be taken into account appropriately. For this purpose, based on a rigorous thermodynamic framework (Lei et al., 2014), the authors have extended the chemo-mechanical model of Loret el al. (2002) for saturated homoionic expansive soils to the unsaturated case (Lei, 2015). In this paper, this chemo-mechanical unsaturated model is adopted to simulate the chemo-elastic-plastic consolidation process of an unsaturated expansive soil layer. Logical tendencies of changes in the chemical, mechanical and hydraulic field quantities are obtained.

1 Introduction

Due to their very uncommon characteristics such as extremely low hydraulic permeability and high swelling capacity, expansive clays are widely used as sealing materials in geotechnical and geo-environmental engineering. However these clays are sensitive to pore water chemical compositions and matric suction changes. Coupled chemo-hydro-mechanical analysis are therefore required to evaluate the mechanical stability and sealing ability of these barriers during the whole life cycle of the engineering works concerned.

To address this complex problem, theoretical developments, based on the rigorous thermodynamic framework [1], were undertaken [2-4] to extend the chemomechanical model [5-6] for saturated expansive clays to account for partial saturation and suction effects. There have been other attempts following different lines of reasoning to model chemomechanical couplings [6-8], but due to limited space are not cited nor analysed here.

2 Soil structure of unsaturated smectite

The properties of unsaturated expansive soils are strongly related to their special soil structures. A typical representative structure for these soils can be described at two structural levels as shown by Figure 1. At the macroscopic level, the soil is considered as a complex of clay aggregates, separated by inter-aggregate pores filled by either gas or free water; Water in inter-aggregate pores is free to move (free water) and is dominated by capillary forces. Inside each aggregate, the microstructural system consists of several clay particles. Each particle contains several layers. Water can reside in the inter-layers or attach to the surface of these clay particles. Being strongly bonded to the clay particles, this water will not migrate nor evaporate except when subjected to very large forces (absorbed water). Accordingly, they will be treated as parts of solid phase. However, absorbed water and free water can exchange mass with each other to reach a thermodynamic equilibrium state. Here this phase change process is treated as chemical reaction.

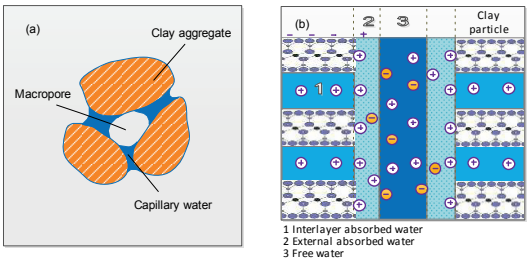

Figure 1. Macro-structure (a) and microstructure (b) of an unsaturated smectite

3 Theoretical framework

3.1 Mixture theory and volume fractions

Mathematically, the unsaturated expansive clay is treated as a three-phase multi-species porous medium. As shown

[a] Corresponding author: KwaiKwan.WONG@entpe.fr
[b] formerly PhD student co-supervised by ENTPE-INSA at the time of this work

in Figure 2, this tri-phasic porous medium, which occupies a volume $d\Omega_t$ in the current configuration, is taken as a representative elementary volume in this work. The solid phase $\mathcal{S}$, liquid phase $\mathcal{L}$, and gaseous phase $\mathcal{G}$ with their respective species can be summarised by the following sets:

$$\mathcal{S}=\{\mathrm{c}',\mathrm{w}',\mathrm{s}_i'\};\mathcal{L}=\{\mathrm{w},\mathrm{s}_i\};\mathcal{G}=\{\mathrm{g}\};\mathcal{F}=\mathcal{L}\bigcup\mathcal{G} \tag{1}$$

where " c' " is the solid clay species, " w " is the water species, " s_i " is the i-th salt species, and " g " is the air species. The superscript " ' " indicates species that are attached to the solid phase, whereas no superscript is used to refer to species within the fluid phases. For example, " w " refers to the free water in the liquid phase, and " w' " refers to the absorbed water attached to the solid phase. " $\mathcal{F}$ " is used to denote the set of species that compose the fluid phases.

To describe the preferential exchange of species between solid phase $\mathcal{S}$ and liquid phase $\mathcal{L}$ that arises from the physical-chemical reactions, a fictitious semi-permeable membrane is assumed to surround the cluster of clay platelets, which is a priori impermeable to clay species c'. However, here the exchange between liquid water and water vapour is neglected by assuming that dry air is the only species in the gaseous phase. To facilitate the frequent reference of the exchangeable species, the following sets of exchangeable species are defined:

$$\mathcal{S}^{\leftrightarrow}=\{\mathrm{w}',\mathrm{s}_i'\};C=\{\mathrm{w},\mathrm{s}_i\} \tag{2}$$

Based on mixture theory, this three-phase porous medium can be treated as the superposition of three continua, one solid and two fluids. These continua are assumed to simultaneously occupy the entire physical domain but with reduced densities to maintain the overall mass balance. The volume fractions (such as porosity n) and saturations (such as the liquid saturation $S_{\mathcal{L}}$ and the gas saturation $S_{\mathcal{G}}$) are introduced to interchange these two densities, as shown in Figure 2. By the same procedure, the multi-species porous medium can also be treated as the superposition of multiple species continua.

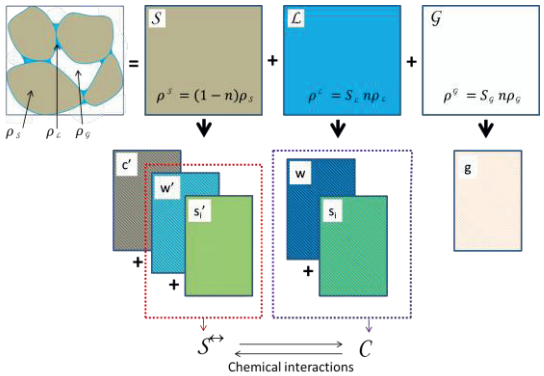

Figure 2. Representation of an unsaturated porous medium as a superimposed mixture: (top) three-phase macroscopic model of the REV; (bottom) multiple-species macroscopic model of the REV.

3.2 Irreversible thermodynamics

Irreversible thermodynamics can provide an efficient description of the coupled processes. Based on energy and entropy balance laws, the Clausius-Duhem inequality associated with the above open thermodynamic tri-phasic clay system consisting of a solid-liquid-gas mixture has been derived in Lei et al. (2014), and is presented by Equation (3). This Clausius-Duhem inequality states that the dissipation Φ of a thermodynamically viable process must be non-negative. For our multi-physical problems, we assume that this dissipation can be decomposed into dissipations associated with mechanical work Φ_m, phase change Φ_{pc}, mass transport Φ_{tr}, and thermal transport Φ_{th}. Each contribution will be required to be positive.

$$\Phi=\Phi_m+\Phi_{pc}+\Phi_{tr}+\Phi_{th}\geq 0 \tag{3}$$

With

$$\Phi_m=\boldsymbol{\sigma}:\frac{d^s}{dt}\boldsymbol{\varepsilon}+\sum_{k\in F}\mu_k\frac{d^s}{dt}m_k+\sum_{k'\in S^{\leftrightarrow}}\mu_{k'}\frac{d^s}{dt}m_{k'} \tag{4}$$

$$-\eta\frac{d^s}{dt}T-\frac{d^s}{dt}\Psi\geq 0$$

$$\Phi_{pc}=-\sum_{\substack{k\in C\\ k'\in S^{\leftrightarrow}}}\left(\mu_k-\mu_{k'}\right)\hat{m}_k\geq 0 \tag{5}$$

$$\Phi_{tr}=-\sum_{k\in F}\boldsymbol{I}^k\cdot\left[\nabla\mu_k+\eta_k\nabla T\right]\geq 0 \tag{6}$$

$$\Phi_{th}=-\frac{q\cdot\nabla T}{T}\geq 0 \tag{7}$$

where, $\boldsymbol{\sigma}$ and $\boldsymbol{\varepsilon}$ are the Cauchy stress tensor and the linearized strain tensor, respectively; m_j and $\hat{m}_j$ are the mass content and the mass growth rate of species j per unit initial volume $d\Omega_0$; μ_j is the chemical potential per unit of mass of species j; η is the total entropy per unit of overall volume of porous medium, T is the absolute temperature, q is the heat flux vector, and Ψ is the total Lagrangian free energy.

4 Model development

In what follows, a set of constitutive relationships under isothermal conditions ($\Phi_{th}=0$) will be formulated. These formulations include a chemo-elastic-plastic model for unsaturated soil skeleton, an unsaturated flow model, and a model of phase change kinematics.

4.1. Chemo-elastic-plastic model

4.1.1 Energy distribution

The dissipation Φ_m is the mechanical dissipation associated with the fluid phases and the solid skeleton, from which, the constitutive models for solid deformation can be derived. To arrive at the formulation of the solid skeleton, we decompose the total free energy Ψ and the

total entropy η into two parts, one associated with the apparent solid skeleton and the other with the bulk fluids. By subtraction, the corresponding parts concerning the apparent solid skeleton can be obtained.

$$\Psi_S = \Psi - \sum_{\alpha=L,G} \Psi_\alpha ; \eta_S = \eta - \sum_{\alpha=L,G} \eta_\alpha \tag{8}$$

From the energy point of view, the apparent solid skeleton can be further viewed as comprising the solid skeleton and the interfaces. Each part has its own associated free energy (Coussy, 2004). To proceed, the solid skeleton is assumed to be decoupled from its attached interfaces by assuming the solid skeleton (sol) and the interfaces (int) have their own associated dissipations and free energies:

$$\Phi_m = \Phi_{sol} + \Phi_{\text{int}} ; \Psi = \Psi_{sol} + \Psi_{\text{int}} \tag{9}$$

In what follows, only the constitutive model for solid skeleton deformation will be presented. In addition, free energy Ψ may include the elastic free energy (reversible, indicated by superscript "e") Ψ^e and locked energy Ψ^p (stored during previous irreversible process, for its release must be accompanied by dissipative process, indicated by superscript "p"). Consequently, the free energy can be further decomposed into:

$$\Psi_{sol} = \Psi^e_{sol} + \Psi^p_{sol} \tag{10}$$

Based on the Clausius-Duhem inequality (4), according to the above analysis, the elastic work input stored as elastic free energies for the solid skeleton can be rewritten as (Lei , 2015):

$$d\Psi^e_{sol} = \bar{\boldsymbol{\sigma}} : d\boldsymbol{\varepsilon}^e + \bar{\mu}_{w'} dm^e_{w'} \tag{11}$$

In which, the generalized effective stresses $\bar{\boldsymbol{\sigma}}$ and the effective chemical potential of absorbed water $\bar{\mu}_{w'}$ is defined as (Lei et al., 2014):

$$\bar{\boldsymbol{\sigma}} = \boldsymbol{\sigma} + p^* \mathbf{1}; \ \bar{\mu}_{w'} = \mu_{w'} - \frac{p^*}{\rho_{w'}} \tag{12}$$

With the equivalent pore pressure p^* defined by $p^* = S_L p_L + (1 - S_L) p_G$.

The following Clausius-Duhem inequality should be satisfied at the same time (Lei , 2015):

$$\Phi_{sol} = \bar{\boldsymbol{\sigma}} : d\boldsymbol{\varepsilon}^p + \bar{\mu}_{w'} dm^p_{w'} + \beta_{sol} d\xi_{sol} \geq 0 \tag{13}$$

Where, β_{sol} is the hardening force energetically conjugated to its corresponding hardening variable, and is defined by $\beta_{sol} = -\left(\frac{\partial \Psi^p_{sol}}{\partial \xi_{sol}} \right)_{S_L}$.

4.1.2 Chemo-hyperelastic model

In tri-axial stress state, the strain work expression (11) can be altered accordingly:

$$d\Psi^e_{sol} = \bar{p} d\varepsilon^e_v + q d\varepsilon^e_s + \bar{\mu}_{w'} dm^e_{w'} \tag{14}$$

In which, the effective stresses $\bar{\boldsymbol{\sigma}}$ and strain $\boldsymbol{\varepsilon}$ are replaced with the volumetric strain ε^e_v, equivalent strain ε^e_s, effective stress $\bar{p}$, Mises equivalent stress q. For the construction of the elastic-plastic model, it is more convenient to treat the stresses as independent variables rather than the strains. To this end, the differential of free energy Ψ^e_{sol} can be transformed using a partial Legendre transform as:

$$d\bar{\Psi}^e_{sol}\left(\bar{p}, q, m^e_{w'}\right) = \varepsilon^e_v d\bar{p} + \varepsilon^e_s dq - \bar{\mu}_{w'} dm^e_{w'} \tag{15}$$

which relates the generalised stress variables $\left(\bar{p}, q, \bar{\mu}_{w'}\right)$ to their work-conjugate counterparts, the generalised strain variables $\left(\varepsilon^e_v, \varepsilon^e_s, m^e_{w'}\right)$.

Now let $\bar{p}_0$ denote a small reference value with the pore fluid as distilled water under purely mechanical loading during the elastic deformation, and the slope of an over consolidation line (OCL) is κ^w. After chemical loading, the slope of this OCL becomes κ, and it intersects the original OCL at the point corresponding to the effective stress $\bar{p}_\kappa$. Following Loret et al. (2002), the expression of the skeleton free energy $\bar{\Psi}^e_{sol}$ is assumed as (Lei et al., 2014):

$$\begin{aligned} \bar{\Psi}^e_{sol} &= \bar{p}\kappa^w \ln\frac{\bar{p}_\kappa}{\bar{p}_0} + \kappa\bar{p}\left(\ln\frac{\bar{p}}{\bar{p}_\kappa} - 1\right) + \frac{q^2}{6G} \\ &- \mu^0_{w'} m^e_{w'} - \frac{RT}{d\Omega_0}\left(N_{w'} \ln N_{w'} - N_S \ln N_S\right) \end{aligned} \tag{16}$$

In the above, R is the universal gas constant, $\mu^0_{w'}$ is the reference chemical potential, $\mathcal{M}_{w'}$ is the molar mass of absorbed water, and $x_{w'} = N_{w'} / N_S$ is the molar fraction of the absorbed water species with $N_{w'}$ and N_S denoting the molar quantities of absorbed water species and all solid phase species, respectively, within the original volume $d\Omega_0$. Now, an incremental chemo-hyperelastic constitutive model can be expressed as:

$$\begin{bmatrix} d\varepsilon^e_v \\ d\varepsilon^e_s \\ -d\bar{\mu}_{w'} \end{bmatrix} = \begin{bmatrix} \frac{\partial^2\bar{\Psi}^e_{sol}}{\partial\bar{p}^2} & \frac{\partial^2\bar{\Psi}^e_{sol}}{\partial\bar{p}\partial q} & \frac{\partial^2\bar{\Psi}^e_{sol}}{\partial\bar{p}\partial m^e_{w'}} \\ \frac{\partial^2\bar{\Psi}^e_{sol}}{\partial q\partial\bar{p}} & \frac{\partial^2\bar{\Psi}^e_{sol}}{\partial q^2} & \frac{\partial^2\bar{\Psi}^e_{sol}}{\partial q\partial m^e_{w'}} \\ \frac{\partial^2\bar{\Psi}^e_{sol}}{\partial m^e_{w'}\partial\bar{p}} & \frac{\partial^2\bar{\Psi}^e_{sol}}{\partial m^e_{w'}\partial q} & \frac{\partial^2\bar{\Psi}^e_{sol}}{\partial m^{e\,2}_{w'}} \end{bmatrix} \begin{bmatrix} d\bar{p} \\ dq \\ dm^e_{w'} \end{bmatrix} \tag{17}$$

Based on the fact that elastic coefficient κ is dependent on the mass contents of the absorbed water $m^e_{w'}$, and by assuming that Poisson's ratio is independent of $m^e_{w'}$, after selected arrangement, another form taking $\boldsymbol{\Sigma} = \left[\bar{p}, q, -\bar{\mu}_{w'}\right]^T$ as generalised stress-like

variables and $\boldsymbol{E}^e = \left[\varepsilon_v^e, \varepsilon_s^e, m_{w'}^e\right]^T$ as generalised elastic strain-like variables can be obtained as

$$\dot{\boldsymbol{\Sigma}} = \boldsymbol{D}^e \dot{\boldsymbol{E}}^e \tag{18}$$

With

$$\boldsymbol{D}^e = \begin{bmatrix} D_{uu} & 0 & D_{um} \\ 0 & 3G & 0 \\ D_{mu} & 0 & D_{mm} \end{bmatrix}$$

In which,

$$D_{uu} = \frac{\bar{p}}{\kappa}; D_{um} = -\frac{\bar{p}}{\kappa} \ln \frac{\bar{p}}{\bar{p}_\kappa} \frac{d\kappa}{dm_{w'}^e} = D_{mu};$$

$$D_{mm} = \frac{\bar{p}}{\kappa}\left(\ln \frac{\bar{p}}{\bar{p}_\kappa} \frac{d\kappa}{dm_{w'}^e}\right)^2 + \bar{p}\left(1 - \ln \frac{\bar{p}}{\bar{p}_\kappa}\right)\frac{d^2\kappa}{dm_{w'}^{e\,2}} + \frac{RT}{\mathcal{M}_{w'}} \frac{1}{x_{w'}} \frac{dx_{w'}}{dm_{w'}^e}$$

4.1.3 Elasto-plastic model

Using the Cam-Clay notation, the solid skeleton dissipation (13) can be rewritten as:

$$\Phi_{sol} = \bar{p} d\varepsilon_v^p + q d\varepsilon_s^p + \bar{\mu}_{w'} dm_{w'}^p + \beta_{sol} d\xi_{sol} \geq 0 \tag{19}$$

Based on the above equation, the principle of maximum plastic dissipation implies the following normality flow rule

$$d\varepsilon_v^p = d\lambda \frac{\partial g}{\partial \bar{p}}; d\varepsilon_s^p = d\lambda \frac{\partial g}{\partial q}; dm_{w'}^p = d\lambda \frac{\partial g}{\partial \bar{\mu}_{w'}} \tag{20}$$

where $d\lambda \geq 0$ is the plastic multiplier, and g is the plastic potential. For simplicity, the plastic potential g is set equal to the yield function f introduced below. In addition, equation (19) also leads to the normality flow rule for the hardening variable

$$d\xi_{sol} = d\lambda \frac{\partial g}{\partial \beta_{sol}} \tag{21}$$

Consistent with the classic plasticity theory, it is assumed that a yield surface exists for the unsaturated expansive soil representing the boundary of the elastic region:

$$f = f\left(\bar{p}, q, \bar{\mu}_{w'}, \beta_{sol}\right) = 0 \tag{22}$$

where the choice of the independent arguments are motivated by the dissipation inequality (19). A general form using the generalised variables can be written as

$$\dot{\boldsymbol{\Sigma}} = \left(\boldsymbol{D}^e - \boldsymbol{D}^p\right)\dot{\boldsymbol{E}} \tag{23}$$

During plastic loading, the stress point is always on the yield surface ($f = 0$) and the consistency condition ($df = 0$) should be satisfied at the same time. Following the classic procedure (Coussy, 2004), the plastic stiffness $\boldsymbol{D}^p$ in the above equation can be solved as

$$\boldsymbol{D}^p = \frac{\boldsymbol{D}^e \left[\frac{\partial g}{\partial \boldsymbol{\Sigma}}\right]^t \left[\frac{\partial f}{\partial \boldsymbol{\Sigma}}\right] \boldsymbol{D}^e}{A + {}^t\left[\frac{\partial g}{\partial \boldsymbol{\Sigma}}\right] \boldsymbol{D}^e \left[\frac{\partial f}{\partial \boldsymbol{\Sigma}}\right]} \tag{24}$$

where A is the hardening modulus, and is obtained by (Coussy, 2004)

$$A = -\frac{\partial f}{\partial \beta_{sol}} \frac{\partial \beta_{sol}}{\partial \xi_{sol}} \frac{\partial \xi_{sol}}{\partial \lambda} = \frac{\partial f}{\partial \beta_{sol}} \frac{\partial^2 \Psi_{sol}^p}{\partial \xi_{sol}^{\,2}} \frac{\partial g}{\partial \beta_{sol}} \tag{25}$$

The modified Cam-Clay model is adopted as the base model, with the yield surface:

$$f = \frac{q^2}{M^2 \bar{p}} + \bar{p} - \bar{p}_c = 0 \tag{26}$$

where M is the slope of the critical state line, and $\bar{p}_c$ is the preconsolidation stress which classically depends on the volumetric plastic strain ε_v^p. To account for the influence of suction and pore water chemical concentration, M is assumed to be dependent on pore water salt concentration as addressed by Loret et al. (2002). Concerning $\bar{p}_c$, besides the dependency on volumetric plastic strain ε_v^p, it is also strongly dependent on matric suction s and pore water salt concentration c_s:

$$\bar{p}_c = \bar{p}_{co} \exp\left(\frac{\varepsilon_v^p}{\lambda - \kappa}\right)\left(\frac{\bar{p}_\lambda}{\bar{p}_{co}}\right)^{\left(1 - \frac{\lambda^w - \kappa^w}{\lambda - \kappa}\right)}\left(\frac{\bar{p}_\lambda}{\bar{p}_k}\right)^{\left(\frac{\kappa - \kappa^w}{\lambda - \kappa}\right)} \tag{27}$$

In the above hardening law, $\bar{p}_{co}$, $\bar{p}_k$, $\bar{p}_\lambda$, κ^w and λ^w are material constants, whereas κ and λ evolve with suction s and pore water salinity c_s, and control the evolution of the preconsolidation pressure.

4.2 Diffusion and mass transfer equations

To complete the theoretical model so that it can be applied to heterogeneous porous media, we also need to derive the trasnport equations of different species in the fluid phases. To do this, we need to invoke the non-negativity of the dissipations mentionned in the inequations (5) to (7). This would lead to the classic formulations of the generalised Darcy's law and Fick's law governing pore-water flow and salt diffusion, as well as to a phenomenological kinetic law governing the phase transformation between free and absorbed water. Due to space limit, these developments would not be shown here; they can be found in [2-3].

5 Experimental results and simulations

A few numerical simulations have been performed to verify the consistency, pertinence and accuracy of the theoretical model developed [2]. Concerning the case of hetergeneous porous media, [3] analysed the progressive

intrusion of salt into a soil layer and its consequences ; its results were also compared to that of a previous publication. In this paper, we choose to present some simulations of the experimental data reported in [9-10]. While results are available for both saturated and unsaturated samples, attention here will be uniquely focused on unsaturated ones. On the other hand, the parameters used in the simulations, as summarized in Tables 1 ad 2, were calibrated using both data on saturated and unsaturated samples [3, 4].

	$m_{c'}$ [kg/m^3]	$m_{s'}$ [kg/m^3]	$m_{w'}$ [kg/m^3]	$x_{w'}$	κ^c	λ^c
0 M	240	0	336	0.967	0.013	0.089
6.53 M	240	0	65.573	0.853	0.007	0.080

Table 1. Parameters for interpolation of chemo-mechanical properties at saturated state

$\overline{p}_{co}$ [kPa]	$\overline{p}_{\kappa}$ [kPa]	$\overline{p}_{\lambda}$ [kPa]	s_e [kPa]	k_3	λ_3	β
50	5000	1300	10	1	5	0.084

Table 2. Parameters for chemo-mechanical model

5.1 Test series 1 and results of simulation

Two series of oedometric tests on unsaturated samples were reported in [10]. In the first, samples were prepared by mixing Boom Clay powder with $NaNo_3$ solutions at 3 different concentrations: 0 M, 4 M and 5.4 M, and were brought to an initial suction of 500 kPa. They were then subject to a compression-decompression cycle at constant suction up to a maximum axial stress of 1000 kPa. Results are plotted in Figure 3a.

Similarly to the case of saturated samples, a salinity increase reduces slightly the virgin compressibility λ, while leaving more or less unaffected the compressibility at overconsolidated states κ. The numerical simulations presented in figure 3b also appear reasonably close to experimental results.

5.2 Test series 2 and results of simulation

In the second series of oedometric tests, 2 samples were prepared with distilled water and brought to an initial suction of 500 kPa and an initial stress of 40 kPa. From this initial state and keeping constant suction and zero salinity, sample 1 was simply compressed to 1000 kPa then decompressed to around 50 kPa. By contrast, sample 2 was subject to a mixed chemo-mechanical loading path: (i) compressed to 100 kPa ; (ii) exposed to 6.54 M $NaNo_3$ solution ; (iii) further compressed to 1000 kPa ; (iv) unloaded to 100 kPa ; (v) exposed to distilled water. Results are plotted in Fig 4a.

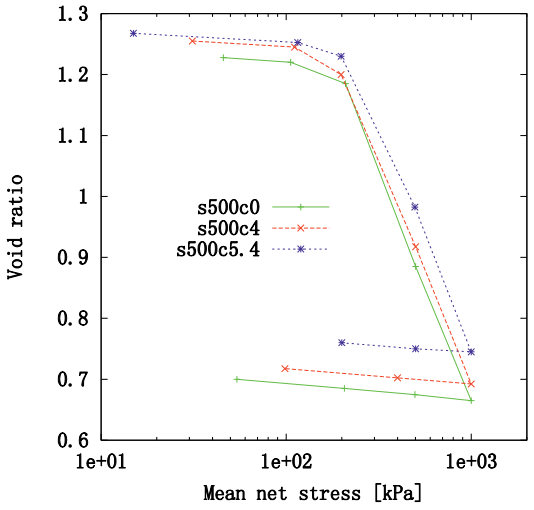

(a) Experimental results

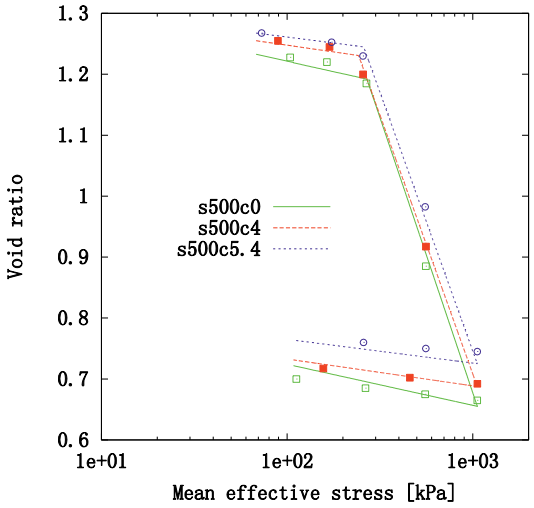

(b) Simulations

Figure 3. Oedometric tests on unsaturated Boom Clay samples (a) experimental data (b) simulations

The tendencies observed are similar to the case of saturated samples [3-4]. A normally consolidated or lowly overconsolidated clay is much more sensitive to salinity changes than a highly over-consolidated clay. This explains why exposure to 6.54 M solution during first compression (close to normally consolidated state) induces a large volume contraction while exposure to distilled water near end of unloading (overconsolidated due to previous compression) has insignificant effects. Chemically-induced plastic collapse in the first case appears to be a logical explanation. Notice also in this regard that the first exposure to 6.54 M solution does induce consistently an increase in the preconsolidation pressure.

Overall, the model seems to reproduce correctly the experimental observations, despite the complexity of the interplay of different mechanisms [4], although some local discrepancies do manifest themselves. In particular, the model appears to overestimate the volume expansion induced by exposure to distilled water at the end of unloading.

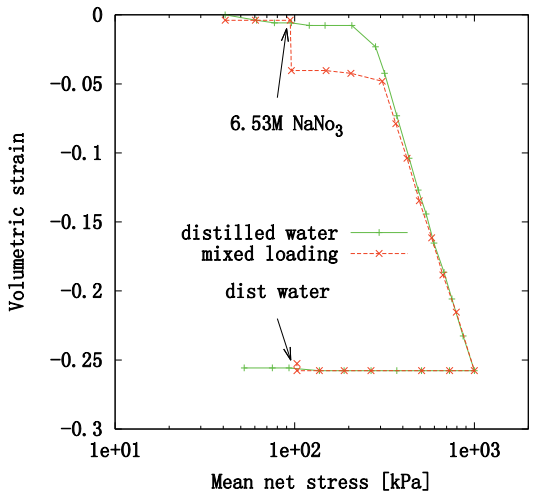

(a) Experimental results

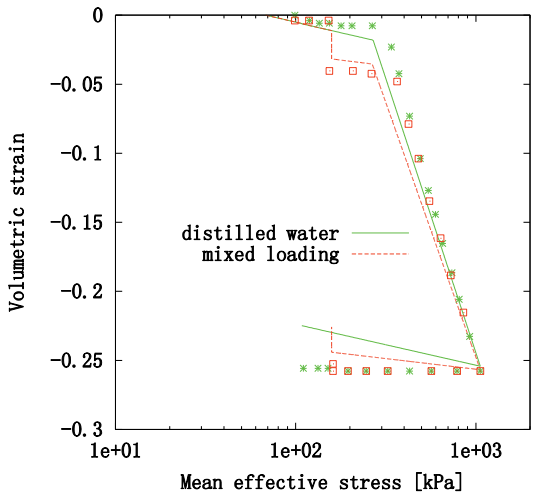

(b) Simulations

Figure 4. Mixed chemical-mechanical loading on unsaturated samples: exposure to 6.53 M solution during loading and to distilled water during unloading, both at vertical stress 100 kPa.

At the present state, the extremely limited amount of experimental data on samples subject simultaneous to suction and chemical loadings does not allow an in-depth analysis of the model which would probably yield ideas on its possible refinements. Further experimentation appears necessary.

6 Conclusion

Based on the modified mixture theory and the theory of non-equilibrium thermodynamics, a theoretical chemo-mechanical model was developed. In this model, the governing equations for chemo-elastic-plastic deformations of unsaturated skeleton, fluid species diffusion and solid-liquid mass transfer have been systematically and rigorously derived. The model was then used to simulate the response of unsaturated soil samples observed during oedometric tests when subject to different chemo-mechanical loading paths. The comparisons globally do not invalidate the model construction while thery also pointed out the necessity for further studies.

References

1. O. Coussy, John Wiley & Sons, Ltd. , (2004)
2. X. Lei, H. Wong, A. Fabbri, A. Limam, Y.M. Cheng, Comput. Geotech. **62** (2014).
3. X. Lei, PhD thesis, INSA-Lyon/ENTPE (2015).
4. X. Lei, H. Wong, A. Fabbri, A. Limam, Y.M. Cheng, I.J.Solids Str., doi:10.1016/j.ijsolstr.2016.01.008 (2016).
5. Loret, B., Hueckel, T., Gajo, A., Int. J. Solids Struct. **39** (2002).
6. Gajo, A., & Loret, B. Comput. Methods Appl. Mech. Eng. **192** (31-32) (2003).
7. L. Guimarães, A. Gens, M. Sanchez, S. Olivella. Geotechique **63**, 2 (2013).
8. Z. Liu, N. Boukpeti, X. Li, F. Collin, IJNAG **29** (2005).
9. N. Mokni, E. Romero, S. Olivella, Geotechnique **64**, (2014).
10. N. Mokni, PhD thesis, Universitat Politècnica de Catalunya (2014).